International Journal of Environmental Science and Technology (2023) 20:4073–4084
https://doi.org/10.1007/s13762-022-04123-w

ORIGINAL PAPER

Photocatalytic degradation of Rhodamine-B by phytosynthesized gold nanoparticles

M. Y. Rather[1] · M. Shincy[1] · SM. Sundarapandian[1]

Received: 11 October 2020 / Revised: 13 November 2021 / Accepted: 14 March 2022 / Published online: 6 April 2022

Abstract

Solving environmental problems by nanoparticles synthesized from plant derivatives has been a prime focus of nanotechnology research. The objective of the present study was to synthesize biogenic gold nanoparticles (AuNP) with dye degradation properties. The influence of mixing ratio of flower extract to metal salt, metal salt concentration and reaction time on nanoparticle size were also explored and optimized for the AuNP formation. For synthesis, flower extract of *Wedelia urticifolia* was added to yellow-coloured gold solutions, and the appearance of cherry red colour in 2 h of contact time demonstrated the fabrication of AuNPs. The synthesized nanoparticles were characterized by UV–Vis spectroscopy, dynamic light scattering (DLS), Fourier transform infrared spectroscopy (FTIR), X-ray diffraction (XRD), and transmission electron microscopy (TEM). Consequently, the nanoparticles were also tested for dye degradation property against Rhodamine-B as a model dye. The strong UV–Visible spectrum peaks at 530–540 nm confirmed the gold nanoparticle synthesis. The DLS results showed the synthesis of the smallest-sized nanoparticles at a 1:1 volume ratio of 1 mM metal solution to flower extract. The FTIR results revealed that proteins and polyphenols help in the reduction and stabilization of synthesized nanoparticles. The XRD analysis indicated that the nanoparticles synthesized were pure and crystalline. Besides, the TEM images displayed spherical particles of size less than 20 nm. The sunlight-driven Rhodamine-B degradation experiments reveal that the dye degradation is dependent on nanoparticle dosage, contact time, as well as pH of dye solution, and more than 90% of dye degradation can be achieved with an AuNP dosage of 20 mg/10 ml of dye solution, pH 3, and a contact time of 15 min. Further, the synthesized nanoparticles can be reused for up to 4 cycles for dye degradation. Hence, the current study quantifies a sustainable and eco-friendly technology for producing AuNPs with fast Rhodamine-B degradation ability.

Keywords Metal nanoparticles · Flower extract · Green synthesis · Dye degradation · Water Pollution

Introduction

Gold nanoparticles (AuNPs) synthesis has acquired huge concern from researchers because of their widespread use in various fields like biotechnology, catalysis, chemistry, medicine, and electronics (Kamal et al. 2014). AuNPs, among all nanoparticles, have stable nature, distinctive surface morphologies, and controlled geometry (Grace and Pandian 2007). These properties are size and shape-dependent (Verma et al. 2013), and differently shaped particles possess a different set of properties (Thakor et al. 2011). For example, triangular nanoparticles show attractive optical properties compared to spherical AuNPs (Ganeshkumar et al. 2012).

Differently shaped nanoparticles can be obtained from different methods of synthesis. Nanoparticles, in general, are reported to be synthesized by a range of procedures, which include physical, chemical, and biological ways (Grzelczak et al., 2020). Physical methods are energy-consuming, whereas chemical methods may sometimes produce synthetic toxic metals that pollute the environment (Ravindran et al. 1999). Biological methods are advantageous over physical and chemical methods (Rather and Sundarapandian 2020). The biological synthesis methods use a natural source of reducing agents from prokaryotes to eukaryotes (Iravani 2011). They have recently received tremendous attention because of their safe and eco-friendly nature. Various

Editorial responsibility: Gaurav Sharma.

✉ SM. Sundarapandian
smspandian65@gmail.com

[1] Department of Ecology and Environmental Sciences, Pondicherry University, Puducherry, India

reducing agents used for synthesizing nanoparticles are yeast (Kowshik et al. 2002), bacteria (Lengke et al., 2006), fungi (Kumar et al. 2007), algae (Govindaraju et al. 2009), and plant extracts (Rather et al., 2020). Although all the biological reducing agents are advantageous over the physical and chemical methods, still use of plant extracts is favoured over other reducing agents because the preparation of plant extracts eliminates the elaborate and time-consuming process of growing and maintaining cell cultures.

The capability of plant extracts to reduce metal ions has been an old concept and known from the early 1900s, but it has been used in metal salt reduction practically from the last few decades only (Santhoshkumar et al. 2017). Plant extract-mediated nanoparticles synthesis is a simple process that can be completed at room temperature, and the reaction completion time is just a few minutes to a few hours (Nadeem et al. 2017). Given the growing need for environment-friendly protocols for synthesizing metal nanoparticles, an attempt was made in the present study to synthesize AuNPs using flower extract of *Wedelia urticifolia*. Twice in a year, pruning this plant to promote its growth is carried out, and thus the produced floral waste could be utilized for nanoparticle synthesis at a grander scale with negligible production cost. Consequently, the synthesized nanoparticles by the proposed extract would be very economical relative to other methods available. Hence, these cheap nanoparticles synthesized could help curb out the menace of water pollution.

The AuNPs synthesized in the present study were used to degrade Rhodamine-B (RhB) because synthetic dyes cannot be easily removed by simple processes (Manu and Chaudhari 2002), and also dyes are presently the significant water pollutants (Khan and Malik 2018) as they affect the normal functioning of ecosystem by affecting the aquatic plants and animals (Lellis et al. 2019). Dyes are used for various applications (Habibi and Askari 2011), and the textile industry alone consumes about 60% of the total produced dyes (Jyoti and Singh 2016). The dyes in wastewaters pose severe threats worldwide (Dutta et al. 2014), and therefore, their degradation is mandatory. Various physical, chemical, and biological processes have been used and are usually ineffective and time-consuming (Wesenberg et al. 2003). Among various processes, the usage of metal nanoparticles is regarded as a convenient process (Caudo et al. 2006; Amini et al. 2014). AuNPs are considered excellent catalysts for reduction reactions (Jyoti and Singh, 2016), and dye reduction by bio-synthesized AuNPs is a practical and powerful approach for wastewater treatment. Due to their unique size and shape-dependent properties as well as their inert nature and very high chemical and physical stability, they are among the most prominent and widely studied nanoparticles. AuNPs are actively employed in various environmental remediation applications and their role in photocatalytic degradation and removal of dyes is well known (Sarfraz and Khan 2021). AuNPs synthesized by *Magnusiomyces ingens* cells served as an efficient catalyst for nitrophenol reduction (Zhang et al. 2016). *Parkia roxburghii* leaf-mediated AuNPs were also investigated for photocatalytic degradation of methylene blue and Rhodamine-B dyes, and satisfactory results were achieved (Paul et al. 2016). Similarly, AuNPs synthesized from *Aspergillum sp.* were used for the degradation of aromatic pollutants and azodyes (Qu et al. 2017). AuNPs synthesized from *Pseudoalteromonas lipolytica* were used for the methylene blue and Congo red dye decolourisation with sodium borohydride (NaBH4) as a reducing agent (Kulkarni et al. 2018). Similarly, AuNPs are prepared from Persea americana showed considerable photocatalytic degradation of methylene blue (Kumar et al. 2018). AuNPs synthesized by *Glomus aureum* fungus depicted effective photocatalytic activity for the degradation of methyl orange dye (Ali et al. 2020).

Hence, the present study has reported the synthesis of AuNPs from the flower extract of *W. urticifolia* and their application in Rhodamine-B (RhB) removal from aquatic environments. The parameters, including the concentration of metal salt, the volume ratio of plant extract to metal salt, and the reaction time, were optimized for nanoparticle formation. Moreover, at different adsorbents, pH of dye solution, and contact time, the photocatalytic RhB dye degradation ability of synthesized AuNPs was also investigated.

Materials and methods

Materials

Gold (III) chloride trihydrate, used as a precursor in the present study, was purchased from HiMedia, while Rhodamine-B (RhB) dye was purchased from Sigma-Aldrich. The RhB dye used in the present study had molecular weight of 479.01 g/mol, CAS number 81–88-9 and C.I. No: 45170. Throughout the experimentation, double-distilled water was used to prepare the plant extract and an aqueous metal salt solution. Flowers were collected from Pondicherry University Campus (12º 0.97´ N, 79º 51.33´ E), Pondicherry, Tamilnadu, India, during the month of April which is the flowering period of *W. urticifolia*.

Flower extract preparation

The flower extract was prepared as explained in our previous work (Rather and Sundarpandian 2021). The flowers were collected, washed thoroughly with tap water, and then distilled water to remove the debris and accompanying biota. Flower broth was made by heating 10 g of fresh flowers in 100 ml of distilled water at 60 °C. After 30 min of heating, the broth was filtered initially through a muslin cloth and

then centrifuged at 10,000 rpm for 10 min. The clear supernatant was stored in the refrigerator to avoid contamination and decomposition.

Synthesis of Gold nanoparticles (AuNPs)

The AuNPs synthesis was completed in two phases. The objective of phase I was to optimize the synthesis parameters, and the objective of phase II was to synthesize nanoparticles in a large amount based on the optimized parameters for photocatalytic application. In the first phase, a total of 20 ml of the reaction mixture of *W. urticifolia* flower extract and metal salt was prepared in the ratio of 1:9, 2:8, 3:7, 4:6, 5:5, 6:4, 7:3, 8:2, and 9:1 in a 100-ml conical flask. The flasks were swirled for about a minute and then left undisturbed at room temperature until the colour changed. The experimental replicas were conducted at 1 mM, 5 mM, and 10 mM metal salt concentrations. The three parameters, i.e. the concentration of metal salt, the ratio of the volume of metal salt to the volume of flower extract, and contact time, were optimized based on the colour change, UV–Vis (UV) spectroscopy analysis, and dynamic light scattering (DLS). The sample showing a higher absorption in the UV–Vis spectrum and the smallest hydrodynamic size in DLS analysis was considered as the optimized and suitable sample for phase II.

Characterization of AuNPs

The characterization techniques used other than UV–Vis and DLS were X-ray diffraction (XRD), Fourier transform infrared spectroscopy (FTIR), and transmission electron microscopy (TEM). Colloidal solutions of prepared particles were used for characterization in UV–Vis, DLS, and TEM. The nanocolloid solution obtained was centrifuged at 10,000 rpm for 15 min to obtain a pellet of nanoparticles for XRD analysis. The pellet was washed with distilled water a couple of times and finally with ethanol to remove the impurities. The pellet was then dried in an oven overnight at 60 °C followed by calcination at 750 °C in a muffle furnace to remove all organic impurities and then powdered.

FTIR spectra for synthesized gold nanoparticles along with W. *urticifolia* flower extract were recorded to confirm the biomolecules responsible for gold nanoparticle synthesis. For analysis, the obtained nanoparticle colloid was centrifuged at 10,000 rpm for 10 min, and pellet precipitated was transferred to watch glasses and dried at 60 °C overnight in an oven. The dried pellet was powdered and then mixed with KBr to form a tablet which was later analyzed by FTIR-Spectrometer (Thermo Nicolet, Model 6700) from a range of 400 to 4000 cm^{-1}. The biomolecules responsible for the reduction, capping, and stabilization of nanostructures synthesized were determined from this spectrum.

Photocatalytic experiments

The synthesized AuNPs were assessed for the photocatalytic degradation of RhB dye. The powder form of nanoparticles was used. Different doses of AuNPs were dispersed in 10 ml of RhB dye solution (20 mg/L concentration), and the mixture was vigorously agitated in the dark using a magnetic stirrer before exposing it to the visible light to ensure the thorough dispersion of nanoparticles. Controls (10 ml of RhB dye solution without adding the synthesized AuNPs) were run under similar experimental conditions. For measuring the percentage of dye degradation, an aliquot of 3 ml was withdrawn from the treated solution and centrifuged at 10,000 rpm for 5 min, and its absorbance intensity was measured at 555 nm wavelength under UV–Vis spectrophotometer. Equation 1 was used to calculate the percentage of RhB dye degradation (Rather and Sundarapandian 2021).

$$\text{Percentage of dye degradation} = \frac{\text{Initial concentration} - \text{final concentration}}{\text{Initial concentration}} \times 100 \quad (1)$$

Results and Discussion

The gold nanoparticle (AuNPs) synthesis by *Wedelia urticifolia* flower extract was attempted in the present study, and the parameters that affect the nanoparticle size were optimized. The metal salt concentration, the metal salt volume to flower extract volume ratio, and the reaction time were optimized because these parameters affect the shape and size of the synthesized nanoparticles (Dubey et al. 2010; Rather et al. 2020). The other two critical parameters, i.e. temperature and pH, were not optimized because they would have affected the cost-effectiveness of the current methodology. For optimization of the nanoparticle synthesis process, metal salt was added to flower extract in the ratio (v/v) of 1:9, 2:8, 3:7, 4:6, 5:5, 6:4, 7:3, 8:2, and 9:1, and the experiments were replicated for three different metal salt concentrations of 1 mM, 5 mM, and 10 mM. The nanoparticle synthesis was evident from the colour change obtained in the samples.

The average particle size distribution determined by DLS (Zetasizer version 6.12, Malvern Instruments Ltd.) for all 27 samples was obtained (Table 1). It is evident from the data that the nanoparticle size was highly dependent on the metal salt concentration and the mixing ratio of extract to the metal salt. The largest average hydrodynamic size was achieved in 10 mM metal salt concentration, and the

Table 1 Average particle size (nm) distribution (determined by DLS) of all 27 synthesized gold nanocolloidal samples

Metal Salt and Flower extract Ratio	Particle Size Distribution for three different concentrations of salt solution		
	1 mM	5 mM	10 mM
9E:1M	605	358	746
8E:2M	305	271	420
7E:3M	158	124	342
6E:4M	161	122	181
5E:5M	55	107	169
4E:6M	66	115	184
3E:7M	72	129	246
2E:8M	80	140	278
1E:9M	106	345	284

*Hereafter, terms E and M will be used for flower extract and metal salt, respectively

smallest was obtained from 1 mM metal salt concentration. The increase in the amount of flower extract resulted in the increased hydrodynamic size of AuNPs, and the possible cause might be the presence of excessive biomolecules (Lee et al. 2013; Rather et al. 2020). The hydrodynamic size of less than 100 nm was obtained in only four mixing ratios 5E:5M, 4E:6M, 3E:7M, and 2E:8M (E stands for flower extract volume; M stands for metal salt volume) of 1 mM metal salt solution.

In AuNPs synthesized from 1 mM gold chloride solution, cherry red colour formation compared to light yellow in control was observed, which intensified with increased contact time. It is a well-established fact that AuNPs exhibit red colour in the water (Shankar et al. 2004). By decreasing the amount of metal salt, the colour shifted from cherry-red to brown. AuNPs synthesized using flower extract of *Rosa rugosa* exhibited pink-red colour in solution, and on increasing the concentration of flower extract, the colour shifted to reddish pink (Dubey et al. 2010), which supports the present results. Thus, the AuNPs colloids obtained from 1 mM concentrated gold chloride solution were analyzed by UV–Visible spectrophotometer (UV–Visible spectrophotometer, Shimadzu, Japan, UV-2400PC Series) in the scanning range of 400 to 600 nm. The surface plasmon resonance (SPR) bands observed between 530 and 540 nm (Fig. 1) in the present study are attributed to synthesized AuNPs. The results are in agreement with several other recent works in which the authors also obtained SPR bands of synthesized AuNPs in the range of 500 to 550 nm (Siddiqi and Husen 2017). Although 5 out of 9 samples depicted SPR peaks, the maximum absorbance value was achieved in 5E:5 M ratio.

Based on the colour change, DLS measurements, and UV–Vis spectroscopy, 1 mM gold chloride solution was selected as the optimized concentration for the synthesis of AuNPs. Also, the 5E:5 M was the optimized ratio because the smallest particle size in the DLS spectrum and the highest absorbance in UV–Vis spectroscopy were achieved. The DLS spectrum of the 5E:5M ratio (1 mM metal salt concentration) is presented in Fig. 2. The reaction time of the synthesis process was also optimized. Nanoparticle colloid of 5E:5M ratio was prepared and subjected to UV–Vis spectroscopy at different intervals of 10 min to 12 h. A gold chloride solution of 1 mM was run as a control, and it did not depict any peak in the spectrum. The peak for the 5E:5M ratio nanocolloid started in 20 min of reaction time at 536 nm, and it intensified up to 12 h (Fig. 3). The lack of peak intensification (peak saturation) after 12 h could be credited to the stability of synthesized nanoparticles, indicating the completion of the reaction.

Several studies have proposed that pH can also be used for optimization and a test for confirming nanoparticle synthesis

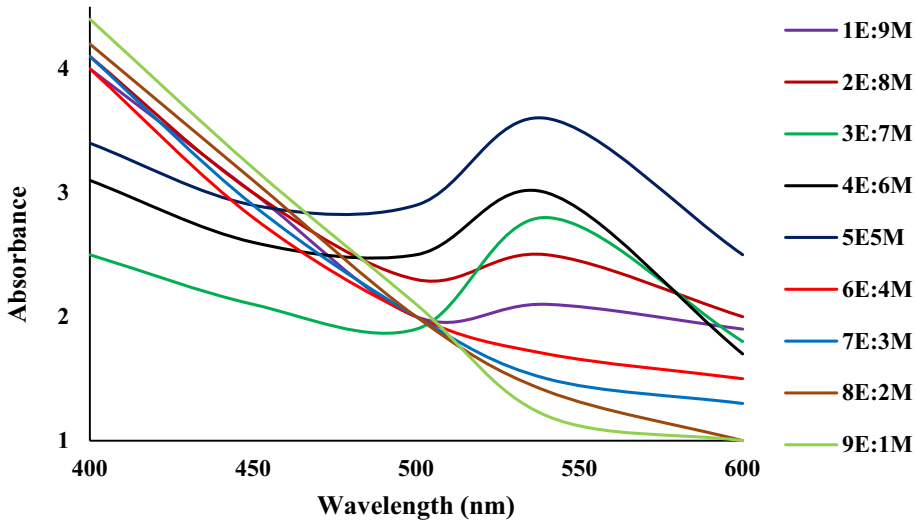

Fig. 1 UV–Visible spectra analysis of AuNPs synthesized at 1 mM concentrated $AuCl_3$ solution

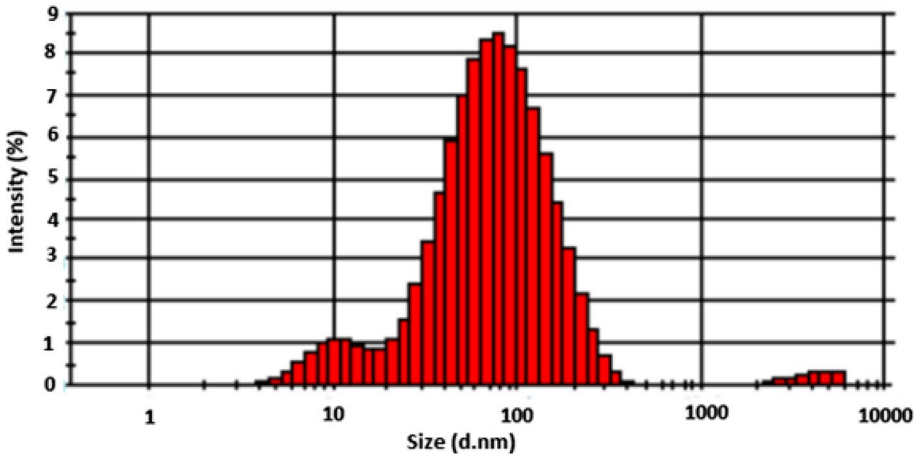

Fig. 2 Dynamic light spectroscopy bar graph of gold nanoparticles synthesized by *Wedelia urticifolia* flower extract ($AuCl_3$ solution concentration 1 mM; ratio 5E:5M)

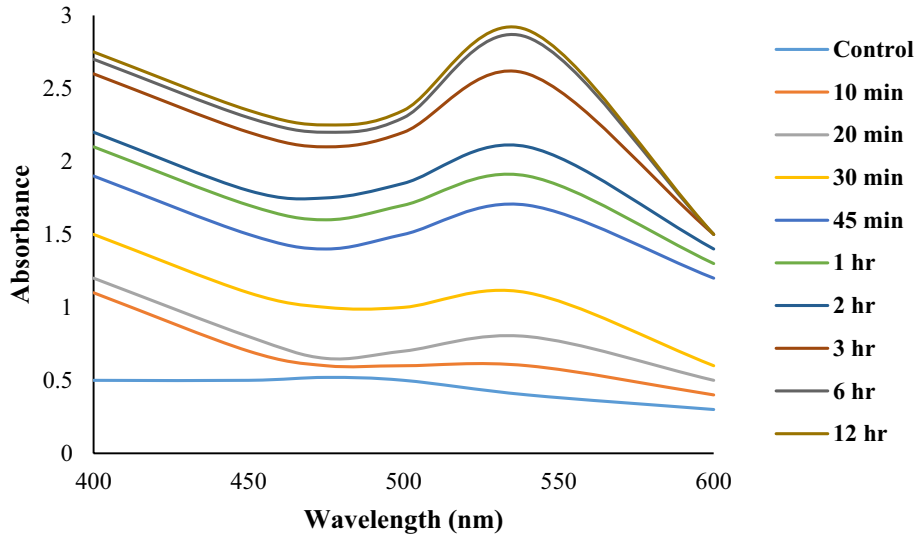

Fig. 3 UV–Visible spectra for time-dependent study of gold nanoparticles synthesized from the optimized sample (1 mM metal salt concentration and 5E:5M v/v ratio)

Table 2 The pH value of gold nanocolloids with reaction time

Reaction time	pH
10 min	4.97
20 min	5.10
30 min	5.17
45 min	5.26
1 h	5.33
2 h	5.57
3 h	5.81
6 h	6.10
12 h	6.18

(Singh and Srivastava 2015; Akintelu et al. 2021). Hence, the pH of the solution was measured at different intervals of time. The results obtained depict that the pH of the AuNPs colloidal solution changes and increases with the contact time (Table 2). It is also clear that the pH values increase from 4.97 to 6.18. The saturation in pH values confirms the stability of synthesized AuNPs. The results are supported by previous findings stating that enhanced AuNP synthesis is observed at pH 6–8 (Umamaheswari et al. 2018; Akintelu et al. 2021). Similar pH change before and after nanoparticle formation was observed in AuNPs synthesized by *Chenopodium formosanum* shell extract (Chen et al. 2019). It was proposed that the change in pH of the iron nanocolloid solution with the reduction of the iron ions indicates nanoparticle formation (Dhuper et al. 2012). Hence, the pH change obtained in the present study also confirms the synthesis of AuNPs.

The FTIR spectroscopy study was carried out to confirm the oxygen functional groups present in flower broth, which could be responsible for the synthesis and stabilization of AuNPs, and the spectra were recorded in the range of 500–4000 cm^{-1} (Fig. 4). The peaks observed at 3403 cm^{-1} and 3324 cm^{-1} AuNPs, respectively, arise due to stretching vibration of the surface hydroxyl group (-OH) of ph^{-1} for flower extract and enolic compounds. Symmetric and

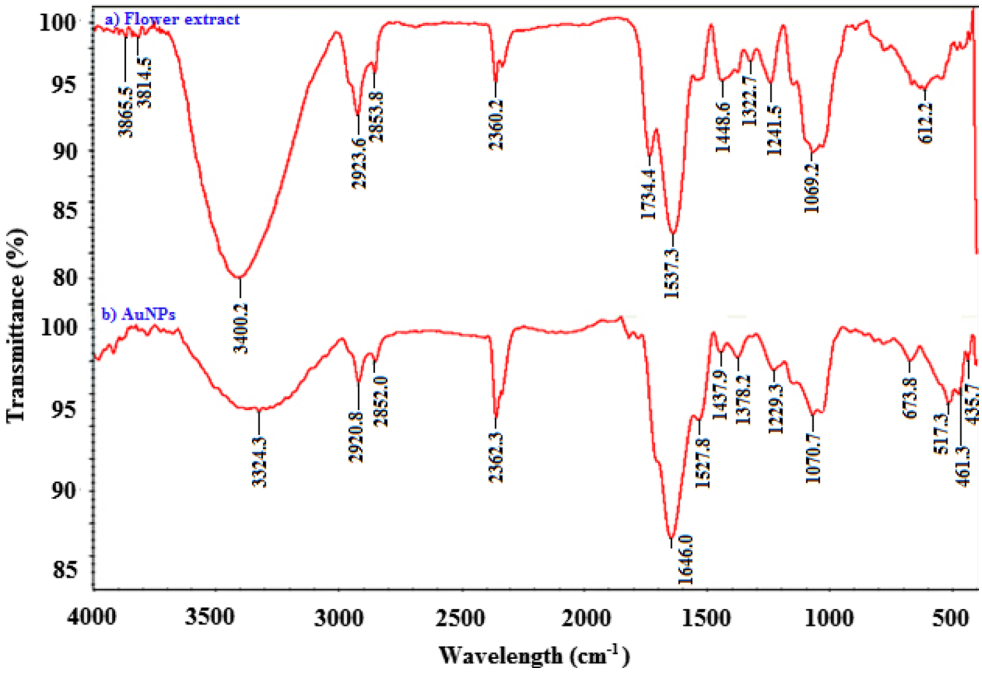

Fig. 4 Fourier transform infrared analysis of flower extract of *Wedelia urticifolia* and synthesized gold nanoparticles

asymmetric $–CH_2$ molecular stretching vibrations give rise to the peaks at 2,923 cm^{-1} and 2,853 cm^{-1} for extract and 2,920 cm^{-1} and 2,852 cm^{-1} for AuNPs (Biswal et al. 2018). The peaks at 1,637 cm^{-1} and 1,646 cm^{-1} are due to the C = O stretching vibration of the amide linkages in proteins (Prakash et al. 2013). Attachment of polyphenolic compounds (flavonoids and terpenoids) to the surface of AuNPs is signified from the 1,440 cm^{-1} and 1,437 cm^{-1} peaks. Absorption peaks at 1,069 cm^{-1} and 1,070 cm^{-1} correspond to C–OH and C-O epoxy groups. The peak at 1,378 cm^{-1} is due to the stretching vibration of the C = C carboxylic group in polyphenols. The peaks at 612 cm^{-1} and 673 cm^{-1} for extract and nanoparticles, respectively, indicate the bending vibrations of the aromatic ring's –CH bond. The peak at 1,734 cm^{-1} in the FTIR spectrum of flower extract results from the carbonyl group of esters indicates that esters may have played a role in the synthesis, capping, or both. Also, a significant shift in C = O and C = C peaks indicates that proteins and polyphenols help reduce and stabilize nanoparticles. The oxidation of aldehydic groups in terpenoids and the absorbance of polyphenolic substances to the surface of the nanoparticles might be responsible for the reduction of metal salt and stabilization of nanoparticles, respectively. The polyphenolic substances absorb on the surface of the nanoparticles by interaction through carbonyl groups or p-electrons (Anuradha et al. 2017).

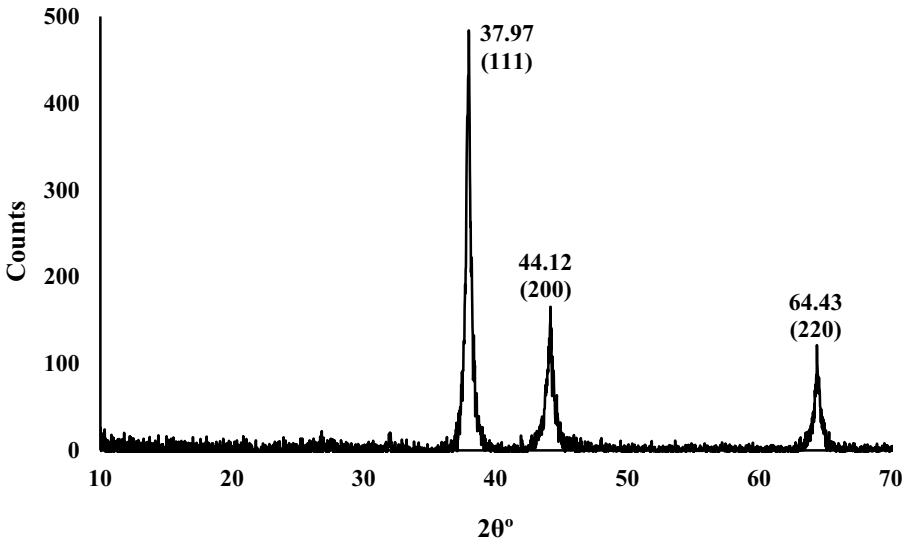

Fig. 5 X-ray diffraction pattern of synthesized gold nanoparticles by *Wedelia urticifolia* flower extract

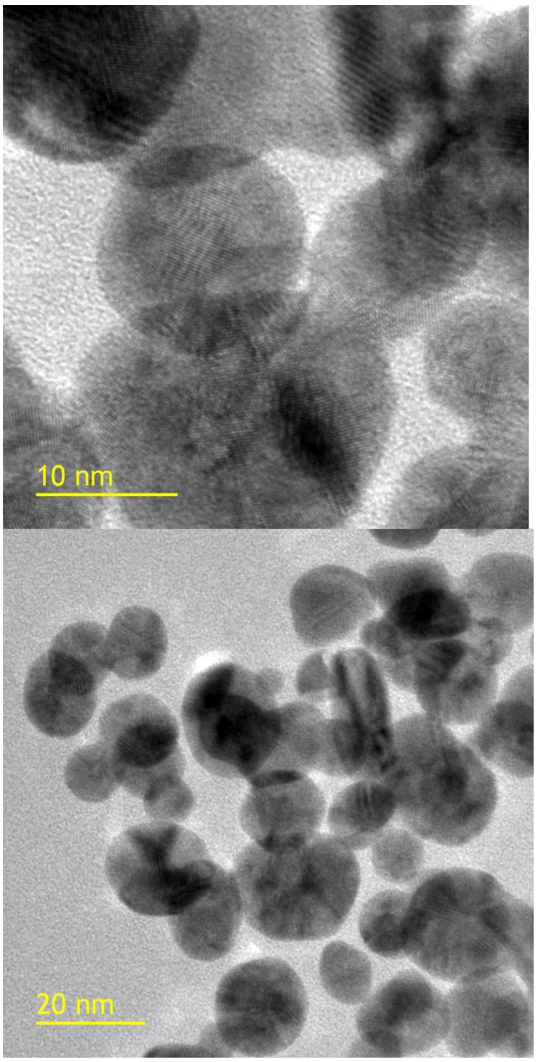

Fig. 6 Transmission electron microscopy images of gold nanoparticles synthesized from *Wedelia urticifolia* flower extract at optimized process parameters

The crystalline nature and structural phase characteristics were confirmed by the X-ray diffraction pattern (Fig. 5). The peaks were obtained at 2θ values of 37.97º, 44.12º, and 64.43º, corresponding to the Braggs diffraction at 111, 200, and 220 planes of the lattice structure, indicating the face-centred cubic (fcc) crystalline structure of the metallic AuNPs (JCPDS: 01–1174). The absence of any sharp peak other than these three peaks confirms the purity of the synthesized AuNPs (Jeong et al. 2009). The XRD peaks obtained in the present study were similar to the results reported earlier (Dubey et al. 2010; Kumar et al. 2011).

The size and the morphology of the synthesized AuNPs were determined by the transmission electron microscopy (TEM, TECNAI-G2 F30-F TWIN). The particles found were spherical and the size calculated using ImageJ software varied between 8.42 and 20.39 nm with an average size of 12.72 nm. The particles are embedded in the biomatrix, as evident from the TEM images (Fig. 6).

The flower extract of *W. urticifolia* reduces the gold salt (Au^{3+}) to AuNPs (Au^{0}). The secondary metabolites present in the extract are responsible for reducing and stabilizing metal nanoparticles because they can donate hydrogen atoms or electrons required to convert to Au^{3+} to Au^{0}. The presence of –OH functional groups in the flower extract is responsible for forming gold complexes, which are then reduced to AuNP seed particles. Similar mechanisms for AuNP synthesis were explained earlier by several other researchers (Muniyappan and Nagarajan 2014; Xiao et al. 2016; Akintelu et al. 2021).

In detail, the photocatalytic degradation of RhB (maximum wavelength at 555 nm) by synthesized AuNPs was investigated. Its degradation was visually evident from the colour change. The degradation was dependent on AuNPs dosage, contact time, and pH of dye solution. The RhB degradation was investigated at three different AuNP dosages

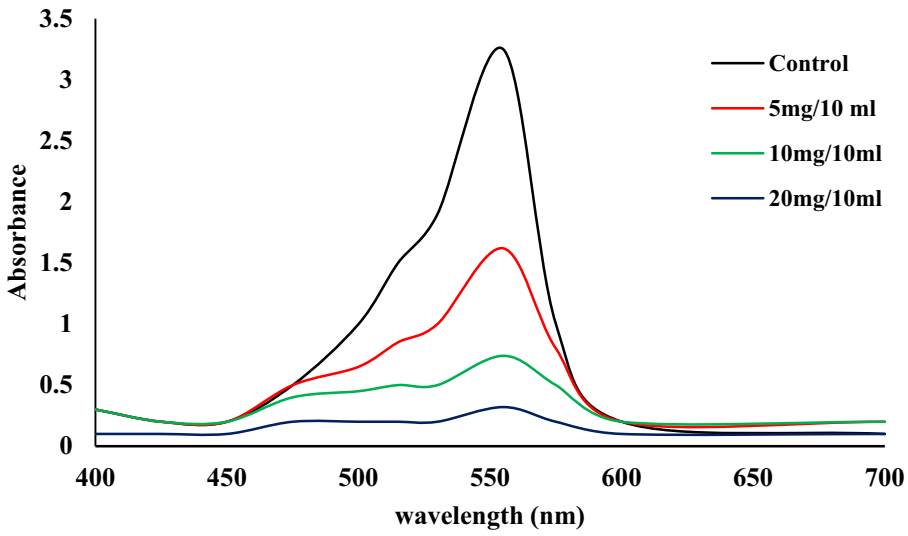

Fig. 7 The effect of synthesized gold nanoparticle dosage on degradation of Rhodamine-b dye (RhB concentration: 20 mg/L; contact time: 20 min)

of 5 mg, 10 mg, and 20 mg per 10 ml of dye solution. It was observed that the degradation increases with an increase in AuNP dosage, and the maximum degradation was achieved at AuNP dosage of 20 mg per 10 ml of dye solution (Fig. 7). Similarly, percentage degradation also increased with the time of contact. The maximum RhB degradation was achieved at 25 min of contact time (Fig. 8). The effect of pH of the dye wastewater on photocatalytic degradation was investigated in detail, and acidic pH was found more favourable compared to the alkaline pH (Fig. 9). The reason for maximum degradation at pH 3 could be the complete protonation of dye as the pKa value for the aromatic carboxylic acid group present on the Rhodamine-B is ~4.2 (Hii et al. 2009; Zhang et al. 2011). Similar results were also achieved by other researchers (Yu et al. 2013). More than 90% of RhB was degraded with AuNPs dosages of 20 mg at pH 3 and a contact time of 15 min.

Photodegradation of harmful dyes using plasmonic photocatalysis has been recently focused (Linic et al. 2011; Wang et al. 2012). The nanoparticles of noble metals like Au have been found to harvest the visible light due to the SPR effect. The SPR directly catalyzes the evolution of hydrogen in the visible region. Recently, the localized surface plasmon (LSP) effect of AuNPs has been used for photocatalysis, giving promising results (Khan and Cho 2019). The electrons of noble metal nanoparticles (for example, AuNPs) are excited by SPR to the conduction band if the incident light wavelength matches the SPR absorption range (Fuku et al. 2013). The SPR properties depend on metal nanoparticles' size, shape, and morphology (Gramotnev and Bozhevolnyi, 2009). The resonant photons interact with the surface electrons, resulting in a high absorption coefficient of photons in resonance with the plasmon excitation and capacitive

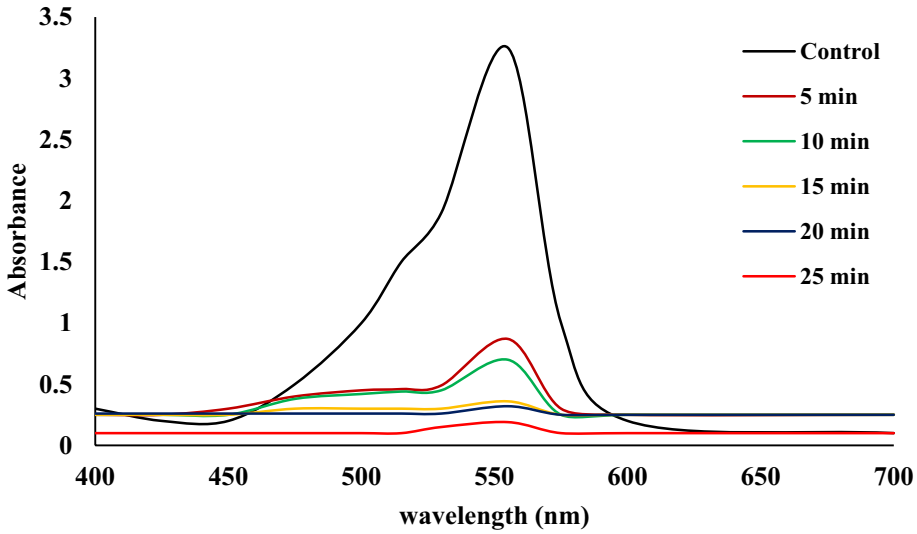

Fig. 8 The effect of contact time on degradation of Rhodamine-b dye by synthesized gold nanoparticles (AuNP dosage: 20 mg/10 ml; RhB dye concentration: 20 mg/L)

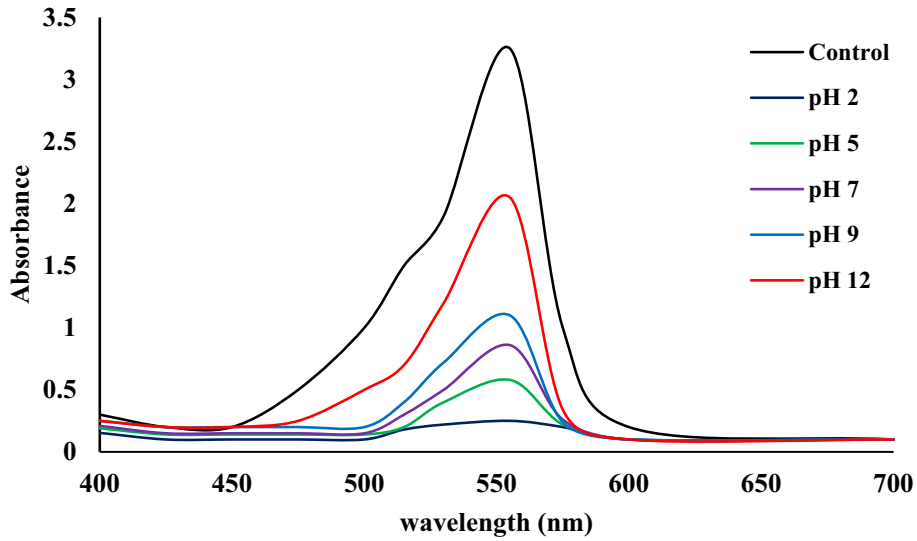

Fig. 9 The effect of pH of solution on Rhodamine-b degradation by synthesized gold nanoparticles (AuNP dosage: 20 mg/10 ml; Rhodamine-b dye concentration: 20 mg/L; contact time: 25 min)

coupling between clusters of plasmonic AuNPs (Khan and Cho 2019).

The primary mechanism of photocatalysis includes the photochemical process using visible light absorption, electron–hole pair generation, separation, and free charge carrier-induced redox reactions. When nanoparticles are irradiated with photons in a photocatalytic degradation, an electron is excited from the valence band to the conduction band, forming a hole, and the excited electrons and holes then migrate to the surface of another state (Linic et al. 2015). Upon photoexcitation, either the photogenerated energetic charge carriers react with the solvent to form highly reactive radicals that can break the chemical bonds of the organic pollutants, or the charge carriers will be transferred directly to the reactants adsorbed on the surface of the catalysts to induce photochemical transformations (Khan and Cho 2019).

The first-order rate equation modelled the degradation kinetics of RhB dye. Moreover, the plot of $\ln(A_t/A_0)$ versus time is depicted in Fig. 10. The kinetic data describe a linear behaviour with an r^2 value of 0.95 and follow the pseudo-first-order rate equation (Jeyapragasam and Kannan 2016; Francis et al. 2017). Based on this model, the rate constant was calculated as 0.067 min^{-1}. The reusability of synthesized nanoparticles for RhB degradation was also investigated. After completing the reaction, the synthesized nanoparticles were separated from the dye solution by centrifugation at 12,000 rpm for 5 min, washed with distilled water, followed by ethanol. The nanoparticle pellet was then dried in an oven at 60 °C for 2 h, powdered using mortar and pestle, and used again for sunlight-driven degradation of RhB. In reusability experiments, the experimental conditions were maintained the same as cycle I. Although from the results, it is clear that synthesized AuNPs could degrade more than 90% of RhB dye in wastewater, there was a significant decrease in percentage dye degradation; the percentage fell below 75% after four cycles (Fig. 11).

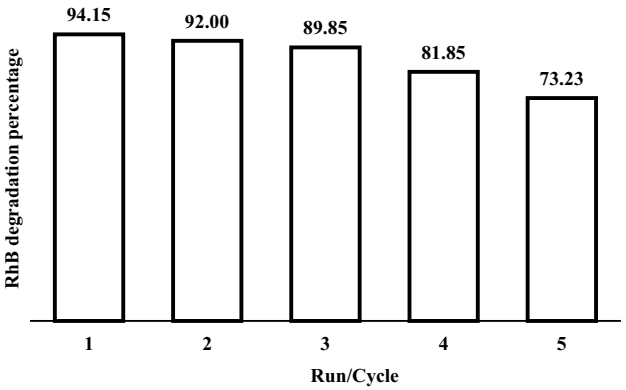

Fig. 11 Reusability of synthesized gold nanoparticles for photocatalytic degradation of Rhodamine-b dye (AuNP dosage: 20 mg/10 ml of dye solution; RhB concentration: 20 mg/L pH: 3; contact time: 15 min)

The possible mechanism of photocatalytic degradation of RhB dye by nanoparticles has been described earlier by several authors, and most of them have suggested that the degradation mechanism is a multistep process that includes photo-absorption, electrons and holes generation, charge carriers transfer, and the recombination of carriers with the dye molecules (Khan et al. 2016; Bishnoi et al. 2018). It was also proposed that the electron–hole recombination gets reduced under the light source, which leads to the enhancement of the interfacial charge transfer reactions (Vijai Anand et al. 2019). Based on their reaction mechanism, analogous projections can be made for the present results as:

$$\text{AuNPs} + h\nu \rightarrow e^-_{CB} + h^+_{VB} \quad (2)$$

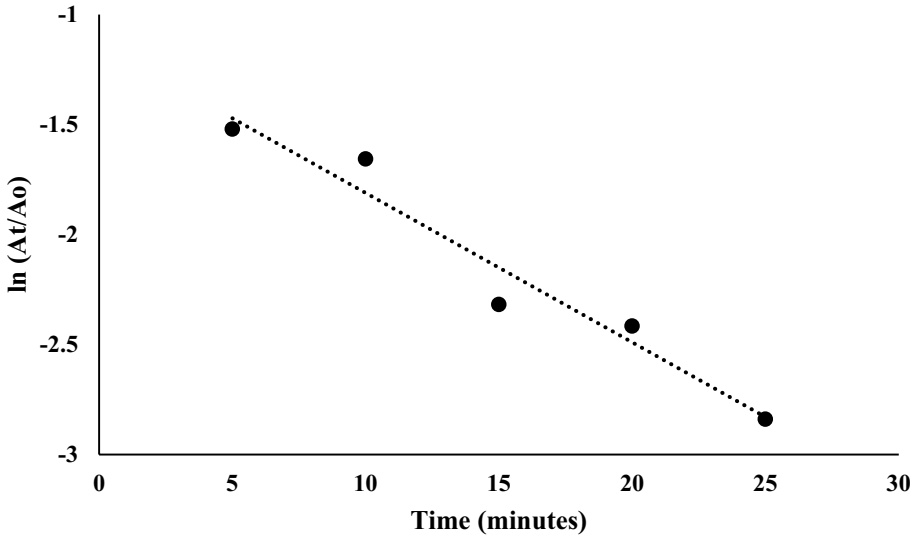

Fig. 10 The plot of $\ln(A_t/A_0)$ versus time for photocatalytic degradation of Rhodamine-b dye by synthesized gold nanoparticles

$$e_{CB}^{-} + O_2 \rightarrow O_2^{-} \quad (3)$$

$$2e_{CB}^{-} + O_2^{1} + 2H^{+} \rightarrow OH + OH^{-} \quad (4)$$

$$h_{VB}^{+} + H_2O \rightarrow H^{+} + OH^{*} \quad (5)$$

$$RhB + OH * \rightarrow \text{Degradation products}\left(CO_2, H_2O, \text{etc.}\right) \quad (6)$$

where *hv* is energy source, e^- is electron, h^+ is hole, CB is conduction band, VB is valence band, and OH* is hydroxyl radical.

A similar mechanism for photocatalytic degradation of norfloxacin using green synthesized silver nanoparticles was suggested earlier (Kanagamani et al. 2019). They proposed that the electrons of synthesized silver nanoparticles excite under visible and move to the lowest unfilled energy band, creating a hole in the valence bond. The process of dye degradation gets completed in several steps. The electrons in the conduction band interact with the ambient oxygen and create the superoxide radical anions. Finally, the superoxide radical anion and norfloxacin react and result in the formation of degradation products. So it can be concluded that the synthesized AuNPs in the present study enhance the production of radical ions, which might assist in the photocatalytic degradation of RhB dye.

Conclusion

The present study concludes that the flower broth of *Wedelia urticifolia* can reduce gold ions into nanoparticles and stabilize them. The synthesized gold nanoparticles depicted peaks in UV–Vis at 530–540, smallest size at a 1:1 volume ratio of 1 mM metal solution to flower extract, pure crystalline structure in XRD, and size of less than 20 nm in TEM. The FTIR results revealed that proteins and polyphenols were responsible for synthesis of nanoparticles. Hence it demonstrates another simple, quick, economical, reproducible, and energy-efficient route of gold nanoparticle synthesis from a very eco-friendly source. The size of gold nanoparticles synthesized varied with the concentration of metal salt used, and the extract added. So, it is advised to optimize such parameters for all plant extract-based nanoparticle synthesis processes. The nanoparticle synthesis method used in this study provides a very prospective methodology for optimization and bulk production of other nanoparticles. The pH change with time is well in agreement with the UV–Visible spectrum taken, and therefore, we suggest that change in pH can be used as a preliminary confirmation for gold nanoparticle synthesis. Furthermore, the photocatalytic dye degradation results revealed reduction of more than 90% Rhodamine-B. The degradation depended on the gold nanoparticles dosage, the pH of the dye solution, and the contact time. Therefore, it can be concluded that the present study offers a different method for the synthesis of pure gold nanoparticles, which can be widely used for the fast removal of dyes from aquatic environments.

Acknowledgements The authors are grateful to the University Grants Commission for providing scholarship during the study period to MYR. The authors are thankful to Central Instrumentation Facility (CIF), Pondicherry University, for proving analytical instrumentation (DLS, TEM, and EDX) for characterization. The authors are also sincerely grateful to the Head, Department of Earth Sciences, Pondicherry University, for XRD characterization.

Data availability Not applicable.

Declarations

Conflict of interest The authors have no conflict of interest to declare.

References

Akintelu SA, Yao B, Folorunso AS (2021) Green synthesis, characterization, and antibacterial investigation of synthesized gold nanoparticles (AuNPs) from *Garcinia kola* pulp extract. Plasmonics 16:157–165. https://doi.org/10.1007/s11468-020-01274-9

Ali S, Ali H, Siddique M, Gulab H, Haleem MA, Ali J (2020) Exploring the biosynthesized gold nanoparticles for their antibacterial potential and photocatalytic degradation of the toxic water wastes under solar light illumination. J Mol Struct 1215:128259. https://doi.org/10.1016/j.molstruc.2020.128259

Amini M, Naslhajian H, Farnia SM (2014) V-doped titanium mixed oxides as efficient catalysts for oxidation of alcohols and olefins. New J Chem 38:1581–1586. https://doi.org/10.1039/C4NJ00066H

Anuradha V, Shankar P, Bhuvan P, Syed AM, Yogananth N (2017) *Terminalia arjuna* bark assisted biosynthesis, characterization and bioactivity of metal oxide nanoparticles. J Chem Pharm Res 9:34–46

Bishnoi S, Kumar A, Selvaraj R (2018) Facile synthesis of magnetic iron oxide nanoparticles using inedible *Cynometra ramiflora* fruit extract waste and their photocatalytic degradation of methylene blue dye. Mater Res Bull 97:121–127. https://doi.org/10.1016/j.materresbull.2017.08.040

Biswal S, Bhaskaran DS, Govindaraj G (2018) Graphene oxide: structure and temperature dependent magnetic characterization. Mater Res Express 5:086104

Caudo S, Centi G, Genovese C, Perathoner S (2006) Homogeneous versus heterogeneous catalytic reactions to eliminate organics from waste water using H_2O_2. Top Catal 40:207–219. https://doi.org/10.1007/s11244-006-0122-6

Chen MN, Chan CF, Huang SL, Lin YS (2019) Green biosynthesis of gold nanoparticles using *Chenopodium formosanum* shell extract and analysis of the particles' antibacterial properties. J Sci Food Agric 99:3693–3702. https://doi.org/10.1002/jsfa.9600

Dhuper S, Panda D, Nayak PL (2012) Green synthesis and characterization of zero valent iron nanoparticles from the leaf extract of *Mangifera indica*. Nano Trends J Nanotech App 13(2):16–22

Dubey SP, Lahtinen M, Sillanpää M (2010) Green synthesis and characterizations of silver and gold nanoparticles using leaf extract of *Rosa rugosa*. Colloids Surf A 364:34–41. https://doi.org/10.1016/j.colsurfa.2010.04.023

Dutta AK, Maji SK, Adhikary B (2014) γ-Fe2O3 nanoparticles: an easily recoverable effective photo-catalyst for the degradation of rose bengal and methylene blue dyes in the wastewater treatment plant. Mater Res Bull 49:28–34. https://doi.org/10.1016/j.materresbull.2013.08.024

Francis S, Joseph S, Koshy EP, Mathew B (2017) Green synthesis and characterization of gold and silver nanoparticles using *Mussaenda glabrata* leaf extract and their environmental applications to dye degradation. Environ Sci Pollut Res 24:17347–17357. https://doi.org/10.1007/s11356-017-9329-2

Fuku K, Hayashi R, Takakura S, Kamegawa T, Mori K, Yamashita H (2013) The synthesis of size-and colour-controlled silver nanoparticles by using microwave heating and their enhanced catalytic activity by localized surface plasmon resonance. Angew Chem Int Ed 125(29):7594–7598. https://doi.org/10.1002/ange.201301652

Ganeshkumar M, Sastry TP, Kumar MS, Dinesh MG, Kannappan S, Suguna L (2012) Sun light mediated synthesis of gold nanoparticles as carrier for 6-mercaptopurine: preparation, characterization and toxicity studies in zebrafish embryo model. Mater Res Bull 47:2113–2119. https://doi.org/10.1016/j.materresbull.2012.06.015

Govindaraju K, Kiruthiga V, Kumar VG, Singaravelu G (2009) Extracellular synthesis of silver nanoparticles by a marine alga Sargassum wightii Grevilli and their antibacterial effects. J Nanosci Nanotechno 19:5497–5501. https://doi.org/10.1166/jnn.2009.1199

Grace AN, Pandian K (2007) Antibacterial efficacy of aminoglycosidic antibiotics protected gold nanoparticles – a brief study. Colloids Surf, A 297:63–70. https://doi.org/10.1016/j.colsurfa.2006.10.024

Gramotnev DK, Bozhevolnyi SI (2009) Plasmonics beyond the diffraction limit. Nat Photonics 4:83–91. https://doi.org/10.1038/nphoton.2009.282

Grzelczak M, Pérez-Juste J, Mulvaney P, Liz-Marzán LM (2020) Shape control in gold nanoparticle synthesis. In: Colloidal synthesis of plasmonic nanometals, Jenny Stanford Publishing, pp 197–220

Habibi MH, Askari E (2011) Photocatalytic degradation of an azo textile dye with manganese-doped ZnO nanoparticles coated on glass. Iran J Catal 1:41–44

Hii SL, Yong SY, Wong CL (2009) Removal of rhodamine-B from aqueous solution by sorption on *Turbinaria conoides* (Phaeophyta). J Appl Phycol 21:625–631. https://doi.org/10.1007/s10811-009-9448-3

Iravani S (2011) Green synthesis of metal nanoparticles using plants. Green Chem 13:2638–2650. https://doi.org/10.1039/C1GC15386B

Jeong GH, Lee YW, Kim M, Han SW (2009) High-yield synthesis of multi-branched gold nanoparticles and their surface-enhanced raman scattering properties. J Colloid Interface Sci 329:97–102. https://doi.org/10.1016/j.jcis.2008.10.004

Jeyapragasam T, Kannan RS (2016) Microwave assisted green synthesis of silver nanorods as catalysts for rhodamine-B degradation. Russ J Phys Chem A 90:1334–1337. https://doi.org/10.1134/S003602441607030X

Jyoti K, Singh A (2016) Green synthesis of nanostructured silver particles and their catalytic application in dye degradation. J Genet Eng Biotechnol 14:311–317. https://doi.org/10.1016/j.jgeb.2016.09.005

Kamal SK, Vimala J, Sahoo PK, Ghosal P, Ram S, Durai L (2014) A green chemical approach for synthesis of shape anisotropic gold nanoparticles. Int Nano Lett 4:109. https://doi.org/10.1007/s40089-014-0109-4

Kanagamani K, Muthukrishnan P, Shankar K, Kathiresan A, Barabadi H, Saravanan M (2019) Antimicrobial, cytotoxicity and photocatalytic degradation of norfloxacin using *Kleinia grandiflora* mediated silver nanoparticles. J Cluster Sci 30:1415–1424. https://doi.org/10.1007/s10876-019-01583-y

Khan ME, Cho MH (2019) Surface plasmon-based nanomaterials as photocatalyst. Advanced Nanostructured Materials for Environmental Remediation. Springer, Cham, pp 173–187

Khan S, Malik A (2018) Toxicity evaluation of textile effluents and role of native soil bacterium in biodegradation of a textile dye. Environ Sci Pollut Res 25:4446–4458. https://doi.org/10.1007/s11356-017-0783-7

Khan H, Khalil AK, Khan A, Saeed K, Ali N (2016) Photocatalytic degradation of bromophenol blue in aqueous medium using chitosan conjugated magnetic nanoparticles. Korean J Chem Eng 33:2802–2807. https://doi.org/10.1007/s11814-016-0238-8

Kowshik M, Vogel W, Urban J, Kulkarni SK, Paknikar KM (2002) Microbial synthesis of semiconductor PbS nanocrystallites. Adv Mater 14:815–818

Kulkarni R, Harip S, Kumar AR, Deobagkar D, Zinjarde S (2018) Peptide stabilized gold and silver nanoparticles derived from the mangrove isolate *Pseudoalteromonas lipolytica* mediate dye decolorization. Colloids Surf, A 555:180–190. https://doi.org/10.1016/j.colsurfa.2018.06.083

Kumar SA, Ansary AA, Ahmad A, Khan MI (2007) Extracellular biosynthesis of CdSe quantum dots by the fungus, *Fusarium oxysporum*. J Biomed Nanotechnol 3:190–194. https://doi.org/10.1166/jbn.2007.027

Kumar VG, Gokavarapu SD, Rajeswari A, Dhas TS, Karthick V, Kapadia Z, Shrestha T, Barathy IA, Roy A, Sinha S (2011) Facile green synthesis of gold nanoparticles using leaf extract of antidiabetic potent *Cassia auriculata*. Colloids Surf, B 87:159–163. https://doi.org/10.1016/j.colsurfb.2011.05.016

Kumar B, Smita K, Debut A, Cumbal L (2018) Utilization of *Persea americana* (Avocado) oil for the synthesis of gold nanoparticles in sunlight and evaluation of antioxidant and photocatalytic activities. Environ Nanotechnol Monit Manag 10:231–237. https://doi.org/10.1002/1521-4095(20020605)

Lee HJ, Song JY, Kim BS (2013) Biological synthesis of copper nanoparticles using *Magnolia kobus* leaf extract and their antibacterial activity. J Chem Technol Biotechnol 88:1971–1977. https://doi.org/10.1002/jctb.4052

Lellis B, Fávaro-Polonio CZ, Pamphile JA, Polonio JC (2019) Effects of textile dyes on health and the environment and bioremediation potential of living organisms. Biotechnol Res Innov 3:275–290. https://doi.org/10.1016/j.biori.2019.09.001

Lengke MF, Fleet ME, Southam G (2006) Morphology of gold nanoparticles synthesized by filamentous cyanobacteria from gold (I) – thiosulfate and gold (III) – chloride complexes. Langmuir 22:2780–2787. https://doi.org/10.1021/la052652c

Linic S, Christopher P, Ingram DB (2011) Plasmonic-metal nanostructures for efficient conversion of solar to chemical energy. Nat Mater 10:911–921. https://doi.org/10.1038/nmat3151

Linic S, Aslam U, Boerigter C, Morabito M (2015) Photochemical transformations on plasmonic metal nanoparticles. Nat Mater 14:567–576. https://doi.org/10.1038/nmat4281

Manu B, Chaudhari S (2002) Anaerobic decolorisation of simulated textile wastewater containing azo dyes. Biores Technol 82:225–231. https://doi.org/10.1016/S0960-8524(01)00190-0

Muniyappan N, Nagarajan NS (2014) Green synthesis of silver nanoparticles with *Dalbergia spinosa* leaves and their applications in biological and catalytic activities. Process Biochem 49:1054–1061. https://doi.org/10.1016/j.procbio.2014.03.015

Nadeem M, Abbasi BH, Younas M, Ahmad W, Khan T (2017) A review of the green syntheses and anti-microbial applications of

gold nanoparticles. Green Chem Lett Rev 10:216–227. https://doi.org/10.1080/17518253.2017.1349192

Paul B, Bl B, Purkayastha DD, Dhar SS (2016) Photocatalytic and antibacterial activities of gold and silver nanoparticles synthesized using biomass of *Parkia roxburghii* leaf. J Photochem Photobiol, B Biol 154:1–7. https://doi.org/10.1016/j.jphotobiol.2015.11.004

Prakash P, Gnanaprakasam P, Emmanuel R, Arokiyaraj S, Saravanan M (2013) Green synthesis of silver nanoparticles from leaf extract of *Mimusops elengi*, Linn. for enhanced antibacterial activity against multi drug resistant clinical isolates. Colloids Surf, B 108:255–259. https://doi.org/10.1016/j.colsurfb.2013.03.017

Qu Y, Pei X, Shen W, Zhang X, Wang J, Zhang Z, Li S, You S, Ma F, Zhou J (2017) Biosynthesis of gold nanoparticles by *Aspergillum* sp. WL-Au for degradation of aromatic pollutants. Physica E 88:133–141. https://doi.org/10.1016/j.physe.2017.01.010

Rather MY, Sundarapandian S (2020) Magnetic iron oxide nanorod synthesis by *Wedelia urticifolia* (Blume) DC. leaf extract for methylene blue dye degradation. Appl Nanosci 10:2219–2227. https://doi.org/10.1007/s13204-020-01366-2

Rather MY, Sundarapandian S (2021) Facile green synthesis of copper oxide nanoparticles and their rhodamine-B dye adsorption property. J Cluster Sci 23:1–9. https://doi.org/10.1007/s10876-021-02025-4

Rather MY, Shincy M, Sundarapandian S (2020) Silver nanoparticles synthesis using *Wedelia urticifolia* (Blume) DC. flower extract: characterization and antibacterial activity evaluation. Microsc Res Tech 83:1085–1094. https://doi.org/10.1002/jemt.23499

Ravindran TR, Arora AK, Balamurugan B, Mehta BR (1999) Inhomogeneous broadening in the photoluminescence spectrum of CdS nanoparticles. Nanostruct Mater 11:603–609. https://doi.org/10.1016/S0965-9773(99)00346-3

Santhoshkumar J, Rajeshkumar S, Kumar SV (2017) Phyto-assisted synthesis, characterization and applications of gold nanoparticles – a review. Biochem Biophys Rep 11:46–57. https://doi.org/10.1016/j.bbrep.2017.06.004

Sarfraz N, Khan I (2021) Plasmonic gold nanoparticles (AuNPs): properties, synthesis and their advanced energy, environmental and biomedical applications. Chem Asian J 16:720–742. https://doi.org/10.1002/asia.202001202

Shankar SS, Rai A, Ankamwar B, Singh A, Ahmad A, Sastry M (2004) Biological synthesis of triangular gold nanoprisms. Nat Mater 3:482–488. https://doi.org/10.1038/nmat1152

Siddiqi KS, Husen A (2017) Recent advances in plant-mediated engineered gold nanoparticles and their application in biological system. J Trace Elem Med Biol 40:10–23. https://doi.org/10.1016/j.jtemb.2016.11.012

Singh AK, Srivastava ON (2015) One-step green synthesis of gold nanoparticles using black cardamom and effect of pH on its synthesis. Nanoscale Res Lett 10:1–12. https://doi.org/10.1186/s11671-015-1055-4

Thakor AS, Jokerst J, Zavaleta C, Massoud TF, Gambhir SS (2011) Gold nanoparticles: a revival in precious metal administration to patients. Nano Lett 11:4029–4036. https://doi.org/10.1021/nl202559p

Umamaheswari C, Lakshmanan A, Nagarajan NS (2018) Green synthesis, characterization and catalytic degradation studies of gold nanoparticles against congo red and methyl orange. J Photochem Photobiol, B 178:33–39. https://doi.org/10.1016/j.jphotobiol.2017.10.017

Verma VC, Anand S, Ulrichs C, Singh SK (2013) Biogenic gold nanotriangles from *Saccharomonospora* sp., an endophytic actinomycetes of *Azadirachta indica* A. Juss Int Nano Lett 3:1–7. https://doi.org/10.1186/2228-5326-3-21

Vijai Anand K, Aravind Kumar J, Keerthana K, Deb P, Tamilselvan S, Theerthagiri J, Rajeswari V, Sekaran SMS, Govindaraju K (2019) Photocatalytic degradation of rhodamine B dye using biogenic hybrid ZnO-MgO nanocomposites under visible light. Chem. Select 4:5178–5184. https://doi.org/10.1002/slct.201900213

Wang P, Huang B, Dai Y, Whangbo MH (2012) Plasmonic photocatalysts: harvesting visible light with noble metal nanoparticles. Phys Chem Chem Phys 14:9813–9825. https://doi.org/10.1039/C2CP40823F

Wesenberg D, Kyriakides I, Agathos SN (2003) White-rot fungi and their enzymes for the treatment of industrial dye effluents. Biotechnol Adv 22:161–187. https://doi.org/10.1016/j.biotechadv.2003.08.011

Xiao Y, Fan J, Chen Y, Rui X, Zhang Q, Dong M (2016) Enhanced total phenolic and isoflavone aglycone content, antioxidant activity and DNA damage protection of soybeans processed by solid state fermentation with *Rhizopus oligosporus* RT-3. RSC Adv 6:29741–29756. https://doi.org/10.1039/C6RA00074F

Yu Y, Murthy BN, Shapter JG, Constantopoulos KT, Voelcker NH, Ellis AV (2013) Benzene carboxylic acid derivatized graphene oxide nanosheets on natural zeolites as effective adsorbents for cationic dye removal. J Hazard Mater 260:330–338. https://doi.org/10.1016/j.jhazmat.2013.05.041

Zhang R, Hummelgård M, Lv G, Olin H (2011) Real time monitoring of the drug release of rhodamine-B on graphene oxide. Carbon 49:1126–1132. https://doi.org/10.1016/j.carbon.2010.11.026

Zhang X, Qu Y, Shen W, Wang J, Li H, Zhang Z, Li S, Zhou J (2016) Biogenic synthesis of gold nanoparticles by yeast *Magnusiomyces ingens* LH-F1 for catalytic reduction of nitrophenols. Colloids Surf, A 497:280–285. https://doi.org/10.1016/j.colsurfa.2016.02.033